PHILOSOPHICAL MAGAZINE B, 1998, VOL. 78, NO. 2, 225–233

Contact and compression of elastic spherical shells: the physics of a 'ping–pong' ball

By L. PAUCHARD† and S. RICA

Laboratoire de Physique Statistique de l'Ecole Normale Supérieure, Unité de Recherche associée au CNRS 1306, Associé aux Universités Paris VI et VII, 24 rue Lhomond, 75231 Paris Cedex 05, France

ABSTRACT

We study the deformation of a thin elastic shell in different situations: case (i) contact with a rigid plane; and case (ii) subject to a localized load. In case (i), experiments show a first-order (discontinuous) transition between two different configurations: the first characterized by flat contact between the shell and the rigid plane and the second by an inversion of curvature leading to contact with the plane along a circular ridge. In addition, the 'slow' impact of an elastic ball presents, qualitatively, a highly anomalous behaviour of the restitution coefficient due to the dissipative energy caused by the friction between the shell and the rigid plane. Case (ii) does not present a transition for small deformations; however, for large deformations on a spherical shell there is a symmetry breaking of the axisymmetric fold shell into corners and polygons to diminish its energy.

§1. INTRODUCTION

One of the most famous problems of contact goes back to the wonderful solution by Hertz of the deformation of elastic bodies when they are compressed against each other. The contact appears as an extreme of the body realizing a singular contact. The problem is to determine the way in which the force is transmitted. Let us describe the Hertz solution briefly. As shown in figure 1, the deformation ϵ happens in a region of linear size $\ell \sim (R\epsilon)^{1/2}$. Therefore, the strain scales as $\partial u/\partial x \sim \epsilon/(R\epsilon)^{1/2} = (\epsilon/R)^{1/2}$, and the total elastic energy stored in the volume (ℓ^3) where the elastic deformation occurs is

$$U \approx E \int dV \left(\frac{\partial u}{\partial x}\right)^2 \sim E\ell^3 \frac{\epsilon}{R} \sim ER^{1/2}\epsilon^{5/2}. \qquad (1)$$

Here, E is Young's modulus. The force $(-\partial U/\partial \epsilon)$ is then proportional to the sesqui-power of the deformation. This nonlinear law comes only from a geometrical factor, for instance in the case of an elastic cylinder in contact with a rigid plate, the elastic energy is quadratic in the deformation: $U \sim EL\epsilon^2$, L being the length of the cylinder taken to be much larger than the radius R.

In this paper we deal with the contact and deformation of elastics shells. We consider them as quasi-two-dimensional elastic sheets, where the thickness, denoted by h, is much smaller than the other two spatial lengths. The theory of plates was established by Föppl (1907) and provides a set of nonlinear coupled partial differential equations, the so-called Föppl–von Kármán equations, which are easier to

†Present address: Laboratoire Fluides, Automatique, Systèmes Thermiques, bâtiment 502, Campus Universitaire, 91405, Orsay Cedex, France.

0141–8637/98 $12.00

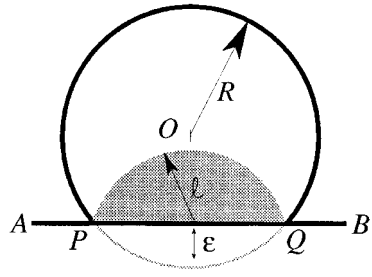

Figure 1. Elastic deformation of a compressed spherical elastic body of radius R. The region where the deformation occurs is of size ℓ and it is drawn in grey. The sphere before deformation is denoted by the grey circle PQ. The linear deformation is denoted by ϵ. The distance PQ is $2\ell = (2R\epsilon)^{1/2}$ to first order in ϵ.

write than to solve. These are valid only for a planar geometry, and a covariant generalization for any curved shell is lacking. However, in the limit of very thick shell some results have been obtained (Ben Amar and Pomeau 1997, Pomeau 1998). The Föppl-von Kármán theory could be applied to shells, if the main deformation is larger than its radius of curvature. In order to consider the shell as a planar sheet, Pauchard *et al.* (1997) found the energy of a deformed spherical shell when the deformation has an axial symmetry.

In §2 we summarize the experiment and theory realized by Pauchard *et al.* (1997). In §3, we describe the dynamical impact of spherical shells and discuss the restitution coefficient. Finally in §4, we study a 'crumpled shell', that is a shell under a large deformation.

§2. Contact of a spherical shell and a plane

In this section, we deal with a situation, rather analogous to the Hertz problem but for shells: the contact between a spherical shell and a rigid plane. Pauchard *et al.* (1994) have discussed recently the compression of a spherical shell (strictly speaking a 'tennis' or a 'ping–pong' ball) in static contact with a rigid plane. This contact reveals some surprises: the existence of a first order transition as the compression increases. We have studied such a transition by the following simple experiment.

Let us consider an hemisphere characterized by its thickness h and its radius R. We studied two types of shells: $h/R \approx \frac{1}{10}$ (tennis balls) and $\frac{1}{50}$ (ping–pong balls). Such an hemisphere is compressed by two parallel rigid plates. The boundary of the half-sphere is fixed to the upper surface in order to eliminate possible non-axisymmetric deformations. The applied load is measured using a dynamometer (figure 2). The experiments lead to two different configurations corresponding to the contact of the shell. For low applied forces, the shell flattens against the horizontal surface with a profile schematized on the left in figure 3 we call this configuration I. For higher compression forces the flattened region buckles upwards as shown on the right in figure 3. This inversion of curvature leads to a circular fold and to a trough: this configuration will be denoted II. The change in behaviour of the shell can be described by the variations in the applied force F as a function of the deformation ϵ (figure 4). Experimental results show that the transition from the flattened to the buckled configuration occurs suddenly, revealing a first-order transition at a deformation ϵ close to twice the thickness h of the shell.

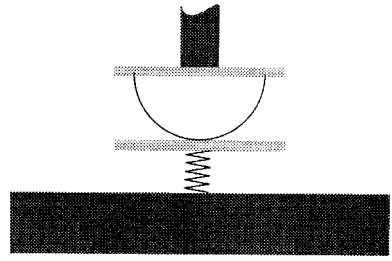

Figure 2. Experimental set-up. The dynamometer is shown as a spring. The boundary of the half-sphere is fixed to the upper surface in order to elimate possible non-axisymmetric deformations.

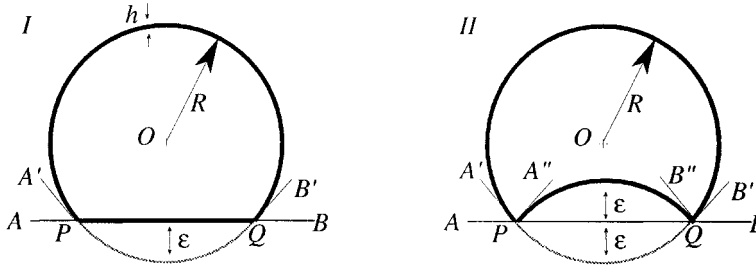

Figure 3. Ideal scheme of the two different configurations of the deformation of a spherical elastic shell of thickness h and radius R. As in the Hertz problem the linear deformation is ϵ. The contact line PQ scales as $\ell \sim (R\epsilon)^{1/2}$.

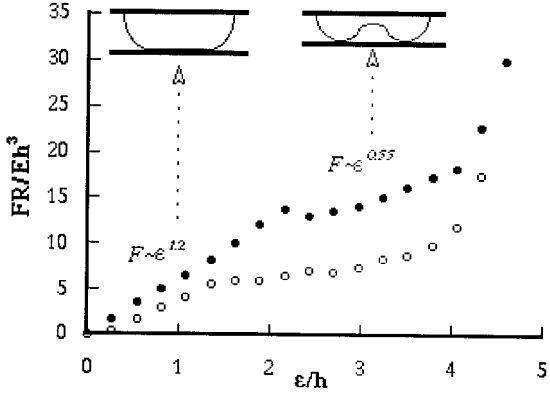

Figure 4. Dimensionless force $(F/Eh^2)(R/h)$ as a function of the deformation (ϵ/h) for a tennis ball. The experimental measurements describe a cycle compression–decomposition revealing a hysteresis loop (●), forward, (○), backward. One notes a sharp transition for $\epsilon/h \approx 2$.

Theoretically, we have estimated the elastic energies for configurations I and II, as a singular perturbation in the limit $h \to 0$ around an idealized deformation (see figure 3) for $h = 0$. We have (Pauchard *et al.* 1997)

$$U_I = \frac{C_0}{4} \frac{Eh^{5/2}}{R} \epsilon^{3/2} + C_1 \frac{Eh}{R} \epsilon^3. \tag{2}$$

$$U_{II} = C_0 \frac{Eh^{5/2}}{R} \epsilon^{3/2} + C_2 \frac{Eh^3}{R} \epsilon. \tag{3}$$

The elastic energy of configuration I is the sum of two contributions. The first term is due to the existence of an axisymmetric circular fold, represented in the figure by the angle A′PQ and PQB′. This energy arises as a balance by between the bending energy and the stretching energy of a plate. The second contribution is the result of the compression of a portion of a sphere (the lighter curve PQ in figure 3), into a planar disc (the bold line PQ in figure 3). The corresponding length change leads to an elastic energy term proportional to ϵ^3. This cubic dependence dominates for large deformations and the force required to make such a deformation increases very quickly, thus, it is not surprising that the system makes a transition to a lower-energy configuration.

The elastic energy of configuration II contains a similar contribution coming from the creation of a circular fold, represented on the right in figure 3 by the angle A′PA″ and B″QB′. The second term in equation (3) comes from the change in elastic energy for the inversion of the spherical section PQ. When one makes such an inversion, the external radius $R + h/2$ becomes an internal radius $R - h/2$; the length change makes an energy contribution linear in the deformation. It is then possible to neglect the second term for $\epsilon \gg h$. However, as we shall see in §4, very large deformations break the axisymmetric circular fold creating polygonal ridges, which minimizes the energy.

For small deformations $U_I < U_{II}$, thus configuration I is energetically favourable; however, as ϵ increases, $U_{II} < U_I$ and configuration II needs a lower elastic energy. There is a critical deformation, roughly proportional to the thickness h (depending on only the Poisson ratio), where the transition arises†. There is no reason for U_I and U_{II} to have the same slope at the transition point. Thus generically there is a jump in the value of the force as observed in experiments. As we deal with a first-order transition, one expects to observe hysteresis. This is indeed observed, even qualitatively. However, this hysteresis is strongly dissipative as shown during the loading–unloading experimental cycle. This dissipation can be determined experimentally by the area enclosed in the loading–unloading cycle (figure 4). We have measured this dissipation for two different sets of experiments consisting of a quasi-static compression of a 'tennis' ball in contact with a dry plate and with a wet (with oil) plate. We have realized different cycles for each set. Those cycles are characterized by two deformations: ϵ_i, which is the transition point to the 'buckled' configuration, roughly equal to 2h, and ϵ_f, which is the maximum of compression. Experimentally, we observe that the area under the hysteresis loop is essentially proportional to the relative displacement $\epsilon_f - \epsilon_i$ (figure 5).

† One may speak of a buckling of the planar disc, represented by the line PQ in figure 3, into an inverted shell; however, one should note that this buckling is subcritical.

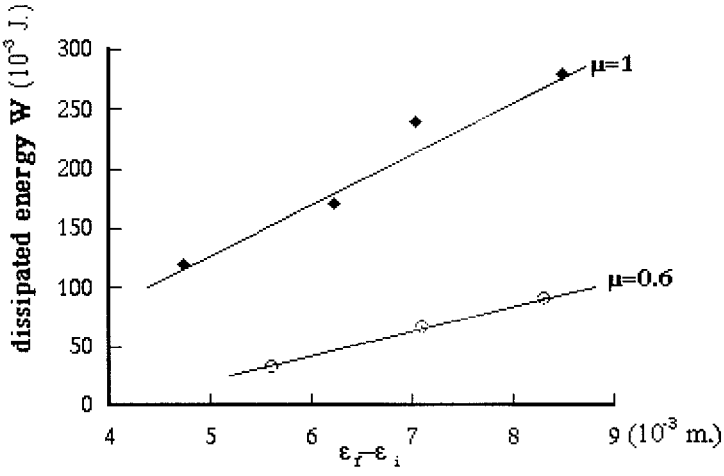

Figure 5. The dissipated energy as a function of $\epsilon_f - \epsilon_i$. The slope is essentially proportional to the friction coefficient (see the text). For both experiments, one gets reasonable values $\mu \approx 1$ for a dry surface (◇) and $\mu \approx 0.6$ for the wet surface (○).

A possible explanation of this dissipation is the following: the circular contact line represented by the points P and Q of configuration II in figure 3 makes a relative displacement respect to the rigid plane AB, creating a mutual friction between the surfaces in contact.

The energy $\mathcal{W}$ dissipated, during the loading–unloading cycle is due to the work of the friction forces. In general, the frictional forces do not depend on the surface contact and are roughly proportional to the normal force (the loading force here). The frictional work is proportional to the normal force and the displacement ℓ. Consequently, the dissipated energy is

$$\mathcal{W} = \mu \int_{\epsilon_i}^{\epsilon_f} \mathrm{d}\left[\left(\frac{R\epsilon}{2}\right)^{1/2}\right]\left(C_0 \frac{3Eh^{5/2}}{2R}\epsilon^{1/2} + C_2 \frac{Eh^3}{R}\right),$$

$$= \mu \frac{Eh^{7/2}}{R^{1/2}}\left(\frac{3C_0}{4\times 2^{1/2}}\frac{(\epsilon_f - \epsilon_i)}{h} + \frac{C_2}{2^{1/2}}\frac{\epsilon_f^{1/2} - \epsilon_i^{1/2}}{h^{1/2}}\right). \qquad (4)$$

For large deformations, one neglects terms in $\epsilon^{1/2}$ and the dissipated energy is proportional to the relative displacement to the transition point in agreement with the experimental results.

§3. Impact of a 'ping-pong' ball: the restitution coefficient

Let us consider now the dynamical contact. First we shall discuss the dynamical approach to the Hertz problem. Let us imagine a projectile, of mass m and speed v_0, impacting on a rigid plate. Ideally, the initial kinetic energy $\frac{1}{2}mv_0^2$ (the body is not yet deformed and thus there is no elastic energy) transforms completely into elastic energy during a time τ_c, to stop the motion of the projectile at a maximal deformation ϵ_{max}. The conservation of energy leads to (Young's

modulus is related to the sound speed of the elastic medium and to its mass density by $E \sim c^2 m/R^3$)

$$\dot{\epsilon}^2 + kc^2 E\left(\frac{\epsilon}{R}\right)^{5/2} = v_0^2, \tag{5}$$

where k is a dimensionless constant depending only on the Poisson ratio. The maximum of deformation scales as

$$\epsilon_{max} \sim R\left(\frac{v_0}{c}\right)^{4/5},$$

and the time during the collision is ($\sim \epsilon_{max}/v_0$)

$$\tau_c \sim \left(\frac{c}{v_0}\right)^{1/5} \frac{R}{c}.$$

Therefore, owing to the 1/5 power pre-factor the collision time is much longer than the time taking by a sound wave to propagate the deformation into the solid (R/c). In this case one might expect the static Hertz solution (1) for the potential energy to a quasistatic process. In this case Hertz' theory gives a satisfactory explanation of the experiments. This quasistatic process could be applied only in few cases; for instance this approximation in not fulfilled in the axisymmetric two-dimensional case of a cylinder, where the contact time does not depend on the amplitude of the maximum of deformation, and $\tau_c \sim R/c$ is roughly the time taken by a sound wave to travel in the section.

The situation for a shell is different; if the initial kinetic energy is low the ball will be compressed only, resulting in configuration I. For larger initial energies the deformation will probably be larger than the critical deformation around 2h in the experiments. Here we shall use only the $\epsilon^{3/2}$ dependence in equation (3), and neglect the friction discussed in §2. From the conservation of mechanical energy one gets

$$\epsilon_{max} \sim \left(\frac{v_i}{c}\right)^{4/3} \frac{R^2}{h}$$

and for the contact time

$$\tau_c \sim \left(\frac{v_i}{c}\right)^{1/3} \frac{R}{h} \frac{R}{c}.$$

Both formulae are valid for $\epsilon_{max} > 2h$, that if $v_0/c > (h/R)^{3/2}$; for the ping–pong balls we have $v_0/c > \frac{1}{325}$, or $v_0 > 1\,m\,s^{-1}$ because $c \approx 320\,m\,s^{-1}$.

In this situation the contact time is sufficiently large with respect to the time which is taken by a sound wave to travel around the spherical shell R/c, because of the factor R/h. This is important because it allows us to use the quasistatic approximation for the dynamic contact, as in the Hertz problem. For smaller speeds, the force law is different. In particular, it grows faster than linearly; thus the contact time diverges as v_0 goes to zero.

We finish this section with a few words about the dissipation created by the friction between the circular fold of the shell and the rigid contact plane. The following considerations are related to the problem of the restitution coefficient of a ping–pong ball. First, if the incident speed is slow, such that $\epsilon_{max} < 2h$, there will be no strong dissipation due to the mutual friction; the only possible mechanism of dissipation comes from the material, loss of linearity, fatigue, shock waves, etc. For a

large incident speed, the dissipation comes mostly from the friction between the ball and the table. This strong dissipation diminishes the speed of the incident particle after the collision. The mechanical energy theorem gives

$$v_0^2 - v_1^2 \sim \mu c^2 \left(\frac{h}{R}\right)^{1/2} \left(\frac{v_0}{c}\right)^{4/3}.$$

Since the restitution coefficient is defined by $v_1 = rv_0$, we have

$$1 - r^2 \sim \mu \left(\frac{h}{R}\right)^{1/2} \left(\frac{v_0}{c}\right)^{-2/3}.$$

All the formulae in §§2 and 3 are only applicable for relatively small deformations ($\epsilon \ll R$). For larger compressions or impact speeds the shell is submitted to very strong stresses; the shell 'crumples', making folds and ridges of different kinds. We shall discuss these in §4.

§4. Compression by a localized load

In §15 of the book by Landau and Lifshitz (1967), one finds the solution to the problem of the deformation of a spherical shell under the effect of a localized applied normal load. In a sense, this is the opposite limit to the contact by a rigid plane; the length scale associated with the applied load is much smaller than the radius of curvature of the shell. For a small applied load, the deformation is localized around the single point of application and increases linearly with increasing force. For larger applied loads, a circular fold centred on the point of contact appears. Here the applied force is proportional to the square root of the deformation (Pogorelov 1988). The transition between these configurations is continuous and the $\epsilon^{1/2}$ power law for the force (Pogorelov 1988) is easy to verify experimentally. Here there is not a large dissipation because there is no friction between the shell and the source of the localized load, and the load–unload cycle is more or less reversible.

However, as the deformation is increased, it becomes energetically favourable to create a polygonal structure essentially composed by a number of right ridges (figure 6); each one joined by a corner $A, B, C, \ldots$); a small-scale structure with a very low energy, the *d* cones (Ben Amar and Pomeau 1997). The situation is very similar to the problem of buckling under a large load considered by Pomeau (1998) in this volume.

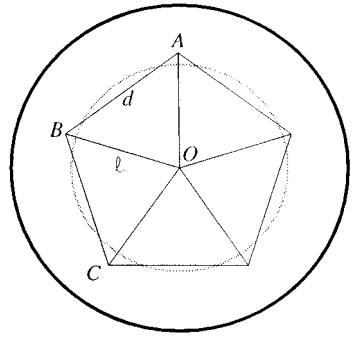

Figure 6. A view from above of the polygonal structure, and the ridges represented as rays from the centre O to the corners $A, B, C, \ldots$ of the polygon.

The energy of the structure has two contributions: the first comes from the polygonal structure which appears at the place of the circular fold; the second contribution comes from the ridges joining the vertex of the polygon to the centre O where the load is applied. Let d be the length of an individual side (e.g. AB and n the number of sides; thus one has $nd \approx \pi(2R\epsilon)^{1/2}$. In the second structure, one has again n ridges but with a length ℓ. The energy of a ridge depends on its length with power 1/3 (Witten and Li 1993) and on the aperture angle with a power 7/3 (Lobkovsky 1996). The aperture angle for the ridges of the polygons is essentially given by the angle A′PA″ of configuration II in figure 3, that is of the order of $(\epsilon/R)^{1/2}$, while for the radial ridges the situation is more complicated. One needs to estimate the angle between the 'planes' OAB and OBC which scales as $\epsilon/(Rn^2)$ when it is small. One may note that 'planes' OAB or OBC are not strictly planes because it costs too much energy to transform a spherical surface OAB or OBC into planes. We consider them as planes in order to estimate the angle of the ridge OB. The corners or d cones do not modify the elastic energy very much. Putting all this together, one gets

$$U(n,\epsilon) \sim Eh^{8/3}R^{1/3}\left[C_1 n^{2/3}\left(\frac{\epsilon}{R}\right)^{4/3} + C_2 n^{-11/3}\left(\frac{\epsilon}{R}\right)^{5/2}\right]. \tag{6}$$

For a large deformation ϵ, the 5/2 power term dominates. Then the energy diminishes on increasing the number of ridges. One needs to compare the energies $U(n,\epsilon)$ with $U(n+1,\epsilon)$ for a fixed ϵ, to see the number of ridges that needs less energy, that is we are interested in $\partial U/\partial n = 0$. Therefore, the number of ridges scales as

$$n \sim \left(\frac{\epsilon}{R}\right)^{7/26}. \tag{7}$$

Thus the number of ridges increases with increasing ϵ just as in experiments (figure 7). It is interesting to note that the number of sides of the polygon do not depend on the thickness h of the shell since ϵ scales with R. We speak here of a very large deformation.

There is another physical system from which it is possible to observe a similar scenario, where an axisymmetric pattern breaks its symmetry into a polygonal structure, namely a hydraulic jump of a viscous fluid (Ellergaard *et al.* 1997).

In the case defined by equation (7) the elastic energy is a function of only the deformation:

$$U \sim Eh^{8/3}R^{1/3}\left(\frac{\epsilon}{R}\right)^{59/39}.$$

Even if the explicit exponent of ϵ is about 3/2 as in equation (3) there is a dimensionless pre-factor proportional to $(h/R)^{7/39}$ which reduces the energy with respect to equation (3) for large deformations. The cross-over deformation between the axisymmetric and the polygonal fold appears when one compares this energy with equation (3), that is

$$\epsilon \sim h^{1/15}R^{14/15}.$$

One gets the force directly from the derivative of the energy (6) and as before, having in mind equation (7),

$$F \sim \frac{Eh^{8/3}}{R^{2/3}}\left(\frac{\epsilon}{R}\right)^{20/39}.$$

In conclusion, 'ping–pong' is easier to play than to understand.

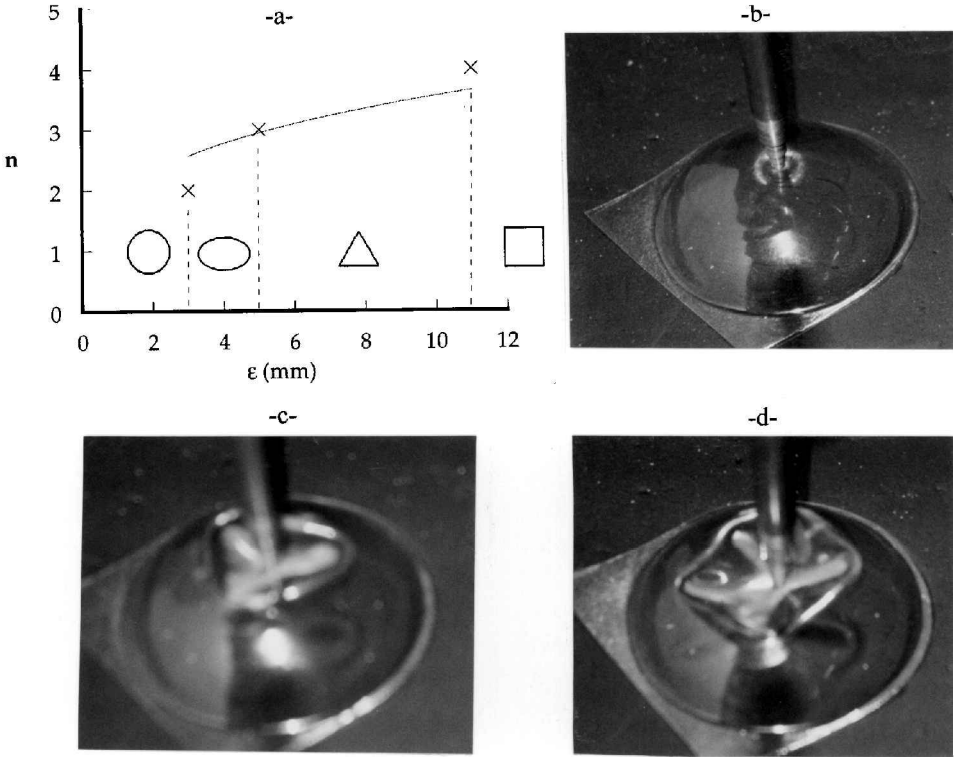

Figure 7. (*a*) Number n of ridges of the polygonal structures versus deformation ϵ. Experimental measurements (X) correspond to the critical deformations at which discontinuous transitions appear between the different structures. The curve displays theoretical predictions. (*b*) Low stress: circular fold centred on the point of contact. (*c*) A polygonal structure displaying three sides and three ridges joining the vertex of the polygon. (*d*) A polygonal structure displaying five sides. The experiments were done using a half-spherical shell (radius 28 mm, thickness 0.17 mm).

Acknowledgements

It is a pleasure to thank Y. Pomeau who outlined this original work. L. Mahadevan for interesting comments, T. Bohr for informing us of the results of Ellergaard *et al.* (1997), and E. Corvera and L. Brouard for their help. Finally, we acknowledge M. Ben Amar, D. Bonn and E. Corvera for inviting us to this summer school, and we thank Cargèse for the beach, cheese, etc., and for the sunsets.

References

Ben Amar, M., and Pomeau, Y., 1997, *Proc. R. Soc.* A, **453**, 729.
Ellergaard, C., *et al.* 1997, *Nature* (submitted).
Föppl, A., 1907, *Vorlesungen tech. Mech.*, **5**, 132.
Landau, L. D., and Lifshitz, E. M., 1967, *Théorie de l'Elasticite* (Moscow: Mir), pp. 83–88.
Lobkovsky, A. E., 1996, *Phys. Rev.* E, **53**, 3750.
Pauchard, L., Pomeau, Y., and Rica, S., 1997, *C. R. hebd. seanc. Acad. Sci., Paris, Sér. II,* **324**, 411.
Pogorelov, A. V., 1988, *Bendings of Surfaces and Stability of Shells* (American Mathematical Society).
Pomeau, Y., 1998, *Phil. Mag.* B, **78**, 235.
Witten, T. A., and Li, H., 1993, *Europhys. Lett.*, **23**, 51.